

This article was downloaded by:

On: 22 January 2011

Access details: *Access Details: Free Access*

Publisher *Taylor & Francis*

Informa Ltd Registered in England and Wales Registered Number: 1072954 Registered office: Mortimer House, 37-41 Mortimer Street, London W1T 3JH, UK



## The Journal of Adhesion

Publication details, including instructions for authors and subscription information:

<http://www.informaworld.com/smpp/title~content=t713453635>

## The Properties of Organosiloxane/Polyester Interfaces at an E-Glass Fiber Surface

A. T. Dibenedetto<sup>a</sup>; S. M. Connelly<sup>a</sup>; W. C. Lee<sup>a</sup>; M. L. Accorsi<sup>a</sup>

<sup>a</sup> Institute of Materials Sciences, University of Connecticut, Storrs, CT, USA

**To cite this Article** Dibenedetto, A. T. , Connelly, S. M. , Lee, W. C. and Accorsi, M. L.(1995) 'The Properties of Organosiloxane/Polyester Interfaces at an E-Glass Fiber Surface', *The Journal of Adhesion*, 52: 1, 41 – 64

**To link to this Article:** DOI: 10.1080/00218469508015185

**URL:** <http://dx.doi.org/10.1080/00218469508015185>

PLEASE SCROLL DOWN FOR ARTICLE

Full terms and conditions of use: <http://www.informaworld.com/terms-and-conditions-of-access.pdf>

This article may be used for research, teaching and private study purposes. Any substantial or systematic reproduction, re-distribution, re-selling, loan or sub-licensing, systematic supply or distribution in any form to anyone is expressly forbidden.

The publisher does not give any warranty express or implied or make any representation that the contents will be complete or accurate or up to date. The accuracy of any instructions, formulae and drug doses should be independently verified with primary sources. The publisher shall not be liable for any loss, actions, claims, proceedings, demand or costs or damages whatsoever or howsoever caused arising directly or indirectly in connection with or arising out of the use of this material.

# The Properties of Organosiloxane/ Polyester Interfaces at an E-Glass Fiber Surface\*

A. T. DIBENEDETTO, S. M. CONNELLY, W. C. LEE and M. L. ACCORSI

*Institute of Materials Sciences, University of Connecticut, Storrs, CT 06269-3136, USA*

*(Received February 9, 1994; in final form May 3, 1994)*

The role of vinylchlorosilane coupling agents in creating an interphase between a polyester matrix and a reinforcing E-glass fiber was investigated. Measurements of the cure kinetics of the polyester resin, using differential scanning calorimetry, revealed that the presence of untreated E-glass surfaces retarded the cure reaction of the polyester, while treatment of the glass with reactive silanes enhanced the cure relative to the unfilled resin. Internal reflection infrared spectroscopy was used to study the permeation of polyester into a polysiloxane coating and the chemical reactions of the vinylsilanes and polyesters. It was found that a vinyltrichlorosilane coupling agent forms a relatively impermeable siloxane film on the fiber surface that probably reacts with the polyester at the siloxane/polyester interface. Octenyltrichlorosilane forms a siloxane layer that is permeated by the polyester and coreacts with it. The resulting interphase is extremely weak and debonds readily from the fiber. Methacryloxypropyltrichlorosilane forms a siloxane layer that is easily permeated by the polyester and reacts with it to form a mechanically-strong interphase. It was also found that the silane surface treatments reduced the stress transmission to the glass fibers, as determined from fiber fragmentation tests, and that the optically observed modes of failure were consistent with the observations of the internal reflection infrared and fiber fragmentation experiments. A finite element analysis of a single fiber embedded in a polymer matrix was used to simulate the effects of interphase toughness and stiffness on the mode of crack propagation from a broken fiber end. While chemical bonding of the interphase to the fiber surface is a necessary condition for a strong, stable interface, it was found that the stress transmission to the fibers (*i.e.*, the fiber efficiency) and the modes of crack propagation are controlled by the stiffness, fracture toughness and the thickness of the applied coatings.

**KEY WORDS** interphase in composites; organosiloxane coatings; curing of polyesters at E-glass surfaces; interphase fracture in composites; finite element analysis of a single fiber composite; internal reflection spectroscopy to study curing at interfaces.

## INTRODUCTION

Silane coupling agents possessing three hydrolyzable groups form three-dimensional multi-layer siloxanes on glass fiber surfaces.<sup>1–3</sup> The morphology of the coating is strongly dependent on the chemical structure of the silane and the method of application. Strong bonding to the glass surface is usually attainable because of the strong

---

\*Presented at the Seventeenth Annual Meeting of The Adhesion Society, Inc, in Orlando, Florida, U.S.A., February 21–23, 1994. One of a Collection of papers honoring Lawrence T. Drzal, the recipient in February 1994 of *The Adhesion Society Award for Excellence in Adhesion Science*. Sponsored by 3M.

interaction of the hydrolyzable groups of the silane with the hydroxyl groups and hydrogen-bonded water on the glass surface, leaving reactive organic groups to interact with the polymeric matrix of the composite. Bonding between a vinyl silane coupling agent and an unsaturated polyester resin, for example, is thought to depend on the potential for copolymerization of the two components. In a typical composite material the siloxane coupling agent thickness may be of the order of 10 to 50 nm, leaving many of the reactive vinyl groups buried within the siloxane network. When an unsaturated vinyl ester is brought into contact with silane-treated glass fibers, the compatibility of the two components will control the wetting of the siloxane surface and the interdiffusion of the two phases. The reaction between the two and the composition and thickness of the resulting interphase depend strongly on the relative reactivity and composition of the components, as well as the processing conditions. It is this interphase that will control the transmission of load to the reinforcing fibers and the mode of failure of the composite materials.

The importance of orientation of the silane functional groups, as it pertains to wettability and chemical reactivity, has been studied by Lee<sup>4</sup> using vinyltrimethoxysilane (VTMS) and  $\gamma$ -methacryloxypropyltrimethoxysilane ( $\gamma$ -MPTMS). For the VTMS, the most probable conformation is vertical orientation of the vinyl functional groups on the glass surface. For the MPTMS, the carbonyl oxygens orient themselves toward the glass surface, hence leaving a silylated surface with characteristics similar to those of unsaturated hydrocarbons.

The effect of silane surface treatment of glass beads on the cure kinetics of an unsaturated polyester resin was studied using  $\gamma$ -MPTMS,<sup>5,6</sup> which is expected to undergo copolymerization with the unsaturated polyester resin, and a phenyltrimethoxy silane (PTS), which is not. Results of the studies show faster reaction rates and higher conversions for the resin with silane-treated glass beads as compared with the resin with untreated glass beads. No significant differences in the cure behavior of the resin filled with  $\gamma$ -MPTMS or PTS-treated glass beads were observed, suggesting that the primary role of the coupling agent is to inhibit the formation of charge transfer complexes *via* effective surface coverage, in agreement with the conclusions of Ishida and Koenig.<sup>7</sup>

There have been a number of investigations of the copolymerization of vinylsilane coupling agents and unsaturated polyester resins.<sup>8-12</sup> In general, it was found that the reactivity of the vinylsilanes in bulk polymerization is highly dependent on the substituents attached to the silicon atom. Furthermore, the reactivity in the presence of glass fiber surfaces is strongly dependent upon the morphology of the silane coating. Koenig and Shih,<sup>12</sup> for example, found significant differences in the copolymerization of vinylsilane (VS) and  $\gamma$ -methacryloxysilane ( $\gamma$ -MPS) with styrene monomer in the interphase.

In any event, it is clear that the chemical reaction between a polyester matrix and a polysiloxane coated fiber is a highly specific phenomenon, depending strongly on the molecular structure of the silane, the coating process, the composition of the polyester and process variables such as temperature and catalyst composition.

The majority of reports in the literature on silane-treated glass fiber reinforced plastics attempt to describe the effectiveness of the silane treatment in terms of the overall macroscopic properties of the composite. The focus of this research is to gain a

better understanding of how the silane coupling agent interphase functions in glass fiber reinforced unsaturated polyesters. In particular, the effects of interpenetration of the polyester into the siloxane coating, the cure kinetics of the polyester resin, and the effects on the stress transferability and resulting failure modes have been investigated.

## EXPERIMENTS

Unsize E-glass fibers with average diameter  $13.0 \pm 0.1 \mu\text{m}$ , untreated E-glass beads with average diameter  $26 \mu\text{m}$ , and fumed silica with specific surface area  $200 \text{ m}^2/\text{g}$  were used as inorganic fillers for an unsaturated polyester resin consisting of a 50:50 mixture of an isophthalic unsaturated polyester (Aropol 7240) and a flexible resin (Aropol 7721) both products of Ashland Chemical Co. Polymerization was initiated by 1 percent by weight benzoyl peroxide.

Vinyltrichlorosilane (VTCS), octenyltrichlorosilane (OETCS), and  $\gamma$ -methacryloxy propyltrichlorosilane (MPTCS) were applied to the fillers from dry hexane solutions containing a large excess of silane, based on monomolecular coverage of the surface. The fillers were dried at  $250^\circ\text{C}$  in vacuum for 24 hours and flushed with dry nitrogen prior to surface treatment with silane. Reactions were carried out at room temperature for 48 hours. The silane-coated glass was washed twice with fresh hexane and dried at  $100^\circ\text{C}$  in vacuum. After drying, the silane-coated glass was washed for 24 hours in a Soxhelt extractor using deionized water to remove physisorbed silane and then redried at  $100^\circ\text{C}$  in vacuum. It is proposed that silylation from an organic solvent is a possible route for obtaining monolayer coverage.<sup>13</sup> Scanning electron micrographs showed a typical "sea island" morphology for the VTCS and OETCS coatings, while the MPTCS deposited as a continuous film with intermittently-spaced micron-sized polysiloxane deposits. A series of samples were prepared to examine the cure kinetics, stress transmissibility and fracture modes in appropriate composite geometries. In addition, stress transmissibility and microscopic studies of fracture modes were carried out using vinylmethylchlorosilane (VMDCS), vinyltrimethylchlorosilane (VTMDCS), octenyltrimethylchlorosilane (OETMDCS) and ethyltrichlorosilane (ECTS).

Differential scanning calorimetry (DSC) was used to investigate the kinetics of the curing of the polyester matrix in composites of 50 percent by weight untreated and treated E-glass beads and fumed silica. Dynamic and isothermal experiments were carried out. Internal reflection infrared spectroscopy (IR-IRS) was used to examine the diffusion and chemical reaction of the unsaturated polyester with the siloxane coatings. The resulting absorption spectra allowed one to follow qualitatively the rate of absorption into the siloxane film, as well as the rate of reaction of the vinyl silane groups. The technique has been described by Garton.<sup>14</sup> Embedded single fiber composites (ESFC) were prepared and fiber fragmentation experiments carried out to measure stress transmissibility of the three siloxane coatings and to observe the modes of interphase and matrix failure. The test procedures are described in a previous publication.<sup>15</sup> A linear elastic axisymmetric finite element analysis (FEA) of an ESFC was performed to determine the effects of fracture toughness, elastic modulus and thickness of an interphase on crack propagation from a broken fiber end. Details of the model are shown in a previous publication.<sup>16</sup>

## RESULTS

### Thermogravimetric Analysis of the Silane Coatings

Thermogravimetric Analysis (TGA) was used to study the thermal stability of the silane coatings as well as the magnitude of the adsorption of the silanes onto the glass bead surfaces. Samples of the silane-coated glass beads were analyzed using a Perkin Elmer Series 7 Thermogravimetric Analyser. The samples were heated from room temperature to 800°C at a heating rate of 20°C/minute under an oxygen atmosphere after which time the total weight loss and onset of rapid degradation were determined.

All coatings appeared to be thermally stable, with no weight loss, up to a minimum temperature of about 300°C. Beyond 350°C there was a rapid degradation of the siloxane, leaving a char of oxidized silicon on the surface at 800°C. Typical char weight ranged from 68.5% for the VTCS films to 35.2% for the MPTCS films. Assuming a uniform coating thickness, we calculated average polysiloxane coating thickness of 130–170 Å for VTCS films, 120–190 Å for OETCS films and 320–460 Å for MPTCS. The average thickness is a function of the coating solution concentration and, since all but the MPTCS films exhibit “sea island” morphology, is only a crude estimate of the thickness of the strongly bonded polysiloxane coatings.

### The Effect of Silane-Treated Surfaces on the Kinetics of Curing an Unsaturated Polyester

Differential scanning calorimetry (DSC) was used to investigate the cure of the unsaturated polyesters in the presence of 50% by weight untreated and silane-treated E-glass beads. Experiments were conducted in both dynamic and isothermal modes using a Perkin Elmer Series 7 DSC. The dynamic experiments were carried out at a heating rate of 5°C/min from 25°C to 250°C. Isothermal experiments were carried out at 90°C, 100°C and 110°C, after an initial ramping of 200°C/min to reach the desired cure temperature. The total heats generated during isothermal and dynamic experiments,  $Q_{\text{iso}}$  and  $Q_{\text{dyn}}$ , were measured and the maximum extent of conversion,  $\alpha_{\text{ult}}(T)$ , obtained isothermally at temperature,  $T$ , was calculated from equation (1).

$$\alpha_{\text{ult}}(T) = \frac{Q_{\text{iso}}}{Q_{\text{dyn}}} \quad (1)$$

It was assumed that the rate of conversion,  $d\alpha/dt$ , is proportional to the rate of heat generated during cure,  $dQ/dt$ , and can be calculated from equation (2), where  $Q_{\text{ult}}$  is the total heat generated during a dynamic run.

$$\left(\frac{d\alpha}{dt}\right)_T = \frac{1}{Q_{\text{ult}}} \left(\frac{dQ}{dt}\right)_T \quad (2)$$

Rate data were analyzed using equation (3), a modified form of a kinetic model suggested by Kamal *et al.*,<sup>17</sup> and extensively used to study the cure of polyesters by Han and Lem.<sup>18–20</sup>

$$\frac{d\alpha}{dt} = k_1(\alpha_{\text{ult}} - \alpha)^n + k_2\alpha^m(\alpha_{\text{ult}} - \alpha)^n \quad (3)$$

The parameters  $k_1$  and  $k_2$  are rate constants, and the quantities  $m$  and  $n$  identify, empirically, the order of the reaction. Consistent with prior literature, we assume  $(m + n) = 2$ .

The total heats of reaction for unfilled, silica-filled and various E-glass bead filled polyesters, determined from dynamic DSC experiments, are all in the range of 330 to 350 J/g and are unaffected by the presence of the fillers. The data are consistent with those previously reported in the literature for similar unsaturated polyesters.<sup>18,21-22</sup>

The extent of conversion,  $\alpha$ , of an unfilled polyester as a function of time and temperature and the reaction rate,  $d\alpha/dt$ , as a function of conversion and temperature, are shown in Figures 1a and 1b, respectively. The maximum rates of conversion are attained within 10 minutes at approximately 15–20 percent conversion in all cases and are strongly dependent upon temperature. Similar results are obtained for the filled polyester systems.

Table I is a summary of the kinetic parameters  $k_1$ ,  $k_2$ ,  $m$  and  $n$  for each of the systems, obtained by a curve fitting of the experimental data. The presence of filler or silane treatment does not appear to have an effect on the order of the reaction; within the reliability of the values obtained by curve fitting,  $m$  and  $n$  remain in the ranges of 0.44 to 0.60 and 1.56 to 1.40, respectively, independent of temperature and the presence of filler. The rate constants  $k_1$  and  $k_2$  increase with temperature and Arrhenius plots yield the activation energies shown in Table II. The calculated values of the rate constants at 90°C and 100°C do not indicate an appreciable effect of glass surface or surface

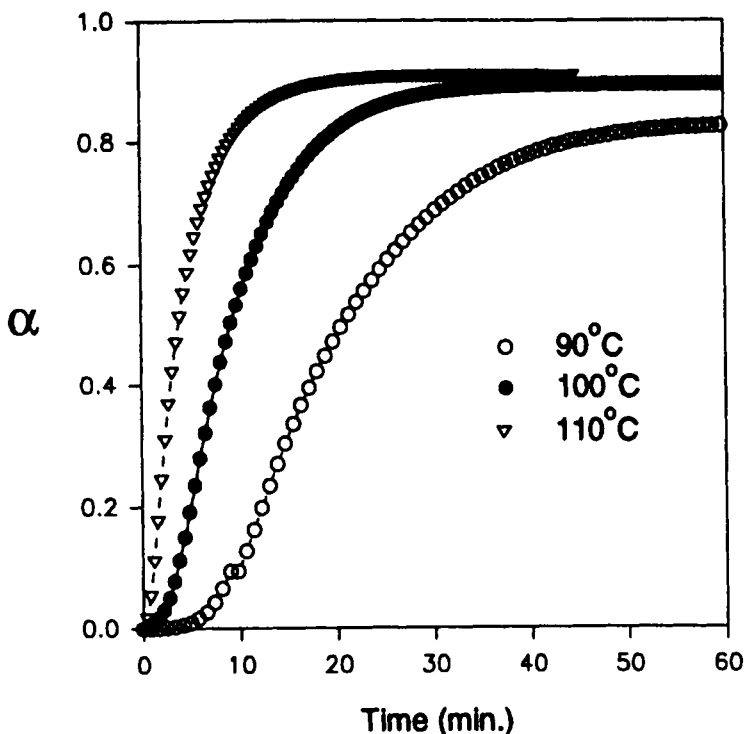


FIGURE 1a Extent of reaction versus cure time for unfilled polyester as a function of cure temperature.

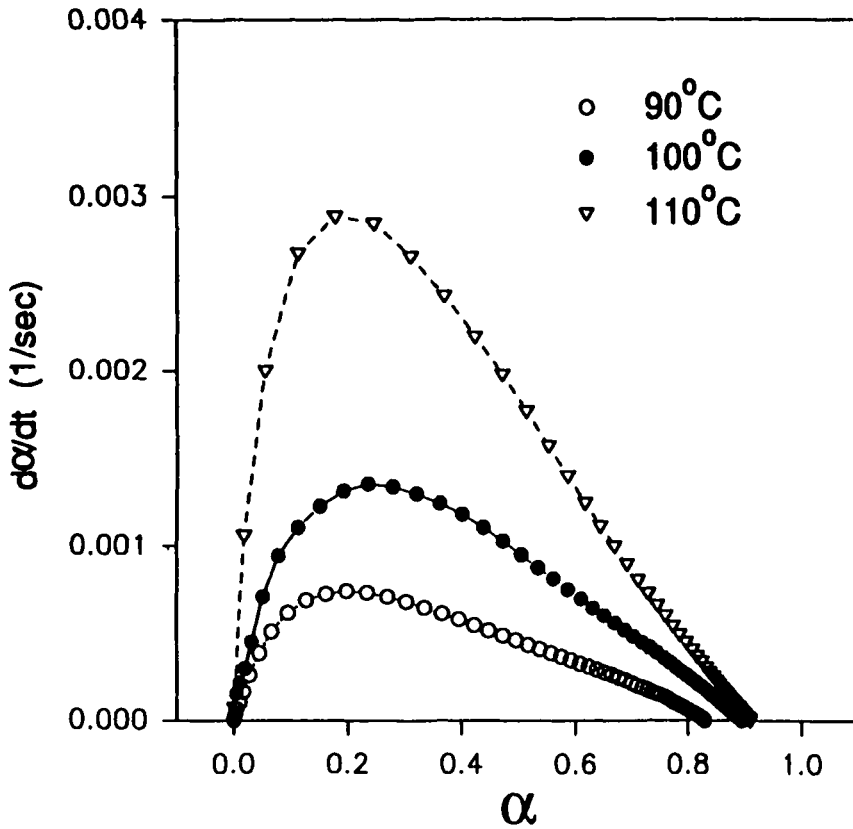


FIGURE 1b Cure rate *versus* extent of reaction for unfilled polyester as a function of cure temperature.

TABLE I  
Kinetic Parameters for Second Order ( $m + n = 2$ ) Reaction of Polyester Cure

System	Temp. (°C)	$k_1 \times 10^4$ (1/sec)	$k_2 \times 10^3$ (1/sec)	$m$	$n$
Unfilled	90	0.10	1.78	0.46	1.54
	100	0.14	4.88	0.55	1.45
	110	1.46	9.39	0.45	1.55
Untreated Glass	90	0.09	1.99	0.52	1.48
	100	0.13	4.62	0.59	1.41
	110	0.60	7.53	0.45	1.55
OETCS	90	0.09	1.77	0.52	1.48
	100	0.13	4.86	0.55	1.45
	110	1.39	8.33	0.44	1.56
VTCS	90	0.10	2.12	0.59	1.41
	100	0.18	5.00	0.55	1.45
	110	1.71	9.23	0.47	1.53
MPTCS	90	0.10	2.69	0.60	1.40
	100	0.37	5.63	0.56	1.45
	110	1.73	8.66	0.45	1.55

TABLE II  
Activation Energies and Correlation Coefficients for Second  
Order ( $m + n = 2$ ) Analysis of Polyester Cure

System	$E_1$ (kJ/gmol)	$R_1^2$	$E_2$ (kJ/gmol)	$R_2^2$
Unfilled Untreated	159.2	0.919	98.6	0.985
Glass	200.7	0.951	92.9	0.991
OETCS	161.3	0.949	92.1	0.995
VTCS	171.6	0.914	87.4	0.984
MPTCS	172.4	0.999	69.4	0.989

treatment on the rates of reaction. At 110°C, however, there is a clear indication that untreated glass surfaces retard the rate of reaction. This effect does not appear to be an artifact caused by the presence of rigid filler. The same experiment using an untreated silica filler of high surface area shows no effect of filler surface on the rate of reaction, as illustrated in Figure 3. The values of  $k_1$  at 110°C also suggest that the VTCS and MPTCS coatings enhance slightly the rate of reaction. This is more clearly illustrated in Figure 2. While the enhancement appears to be real, and consistent with the results of previous

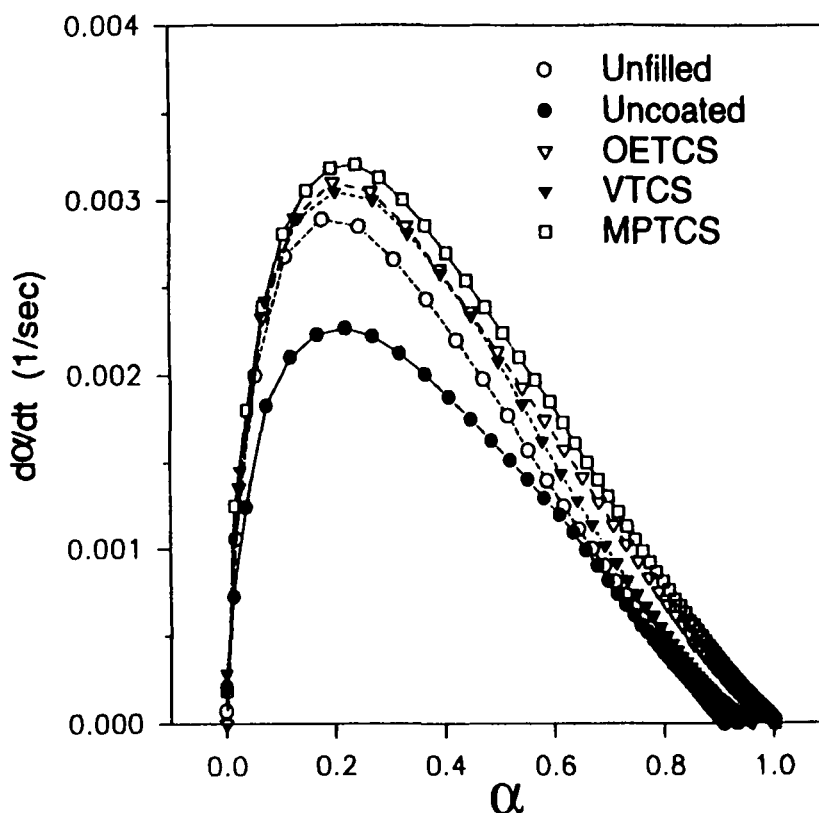


FIGURE 2. Cure rate versus extent of reaction for various silane coated glass bead-filled polyester resins @ 110°C.



investigators,<sup>6</sup> the calculated absolute values of  $k_1$  and  $k_2$  may not be reliable indicators of subtle differences between coatings since it is difficult to define precisely a global minimum in the multi-variable optimization procedure used to calculate the rate constants.

The retardation of cure by bare E-glass surfaces is consistent with the findings of Shieh and Hsiu<sup>22</sup> and Ishida and Koenig.<sup>7</sup> The latter authors attribute this retardation to the formation of charge transfer complexes between the free radicals in the organic phase and the metal oxides on the E-glass surface. The absence of an effect in the presence of pure silicon supports this hypothesis. The magnitude of the enhancement of cure rate in the presence of silane treatments appears to be dependent on the properties of the organofunctional groups of the silane deposited on the surface of the E-glass, the MPTCS-treatment yielding a greater enhancement than those of either the OETCS or VTCS treatments. Differences in the maximum extent of conversion are also observed, with higher degrees of conversion obtained in systems containing silane-treated E-glass. The results are consistent with those of Lee and Han.<sup>6</sup> Thus, in these cases, one should expect the properties of the polyester near the glass surface to be somewhat different from those in bulk.

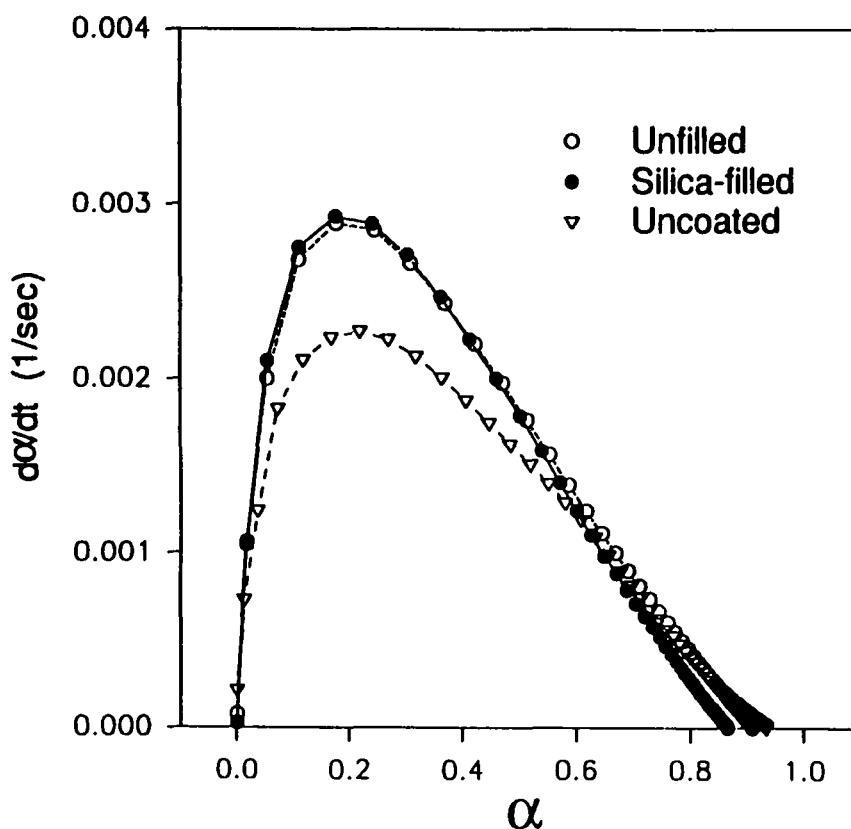


FIGURE 3 Cure rate versus extent of conversion for unfilled, silica-filled, and uncoated glass bead-filled polyester @ 110°C.

### Behavior of the Silanes in the Interphase

Internal reflection-infrared spectroscopy (IR-IRS) was used to study the interaction of the silanes with the unsaturated polyester in the interphase adjacent to an inorganic surface. A  $60^\circ$  parallelogram-shaped germanium crystal ( $50 \times 10 \times 2$  mm) was used because of its wide optical window, among other favorable properties. The technique has been described by Garton<sup>14</sup> and a schematic of the IRS sample geometry is shown in Figure 4. The element is spray-coated twice with a 2% v/v solution of the coupling agent in hexane, and allowed to dry in air at room temperature for 15 minutes, after which it is rinsed twice in distilled water and placed in a vacuum oven at  $100^\circ\text{C}$  for 15 minutes. The experiment was conducted with MPTCS, OETCS and VTCS coatings. The average thickness of the films was determined from the absorbance of a characteristic radiation from each material, using a calibration technique developed by Garton.<sup>24-26</sup> The average thicknesses obtained were  $0.2\ \mu\text{m}$  for MPTCS,  $0.08\ \mu\text{m}$  for VTCS and  $0.06\ \mu\text{m}$  for OETCS films. These were chosen so as to enable the monitoring of both the vinyl groups on the silanes and interactive groups on the polyester. The

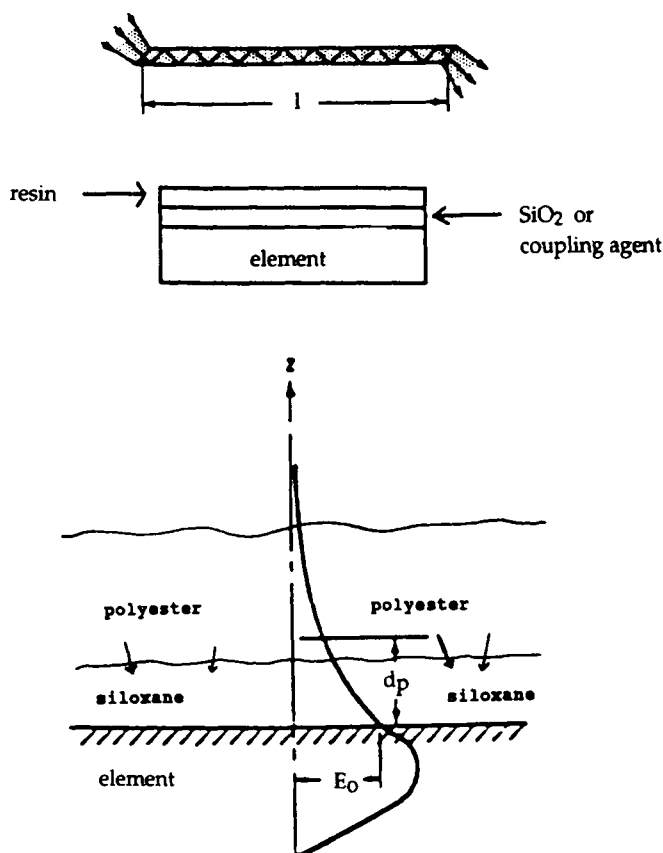


FIGURE 4 Schematic of IRS sample geometry.

depth of penetration of the radiation in the region of the carbon double bond stretching mode was calculated to be of the order of  $0.3\ \mu\text{m}$ , thus enabling both silane and polyester to be visible in the exponentially-decreasing amplitude of the electric field.

The hydrolytic stability of the silane coatings on germanium was determined by immersing the silane-treated elements in boiling water for 30 minutes. Examination of the region between  $1000\ \text{cm}^{-1}$  and  $1200\ \text{cm}^{-1}$  in the spectra reveals a decrease in the peak intensities, indicating a decrease in the amount of polysiloxane on the surface of the germanium. Reductions of 40%, 68% and 65% in the peak intensities were observed for the VTCS, OETCS and MPTCS coatings, respectively. This reduction results from the removal of hydrolyzed silane during the boiling water treatment. In all cases there appears to be a layer of the silane coupling agent that is strongly bonded to the germanium element.

The coated germanium element was placed in a specially designed chamber, heated by a circulating oil bath to the desired temperature, after which a spectrum of the silane coating was taken. A large excess of the unsaturated polyester resin, mixed with benzoyl peroxide initiator, was then injected into the chamber and the cure reaction was monitored for at least one hour.

The spectra at  $90^\circ\text{C}$  as a function of the time that the VTCS coating was in the presence of unsaturated polyester are shown in Figure 5. The intensity of the carbonyl absorption peak of the unsaturated polyester at  $1726\ \text{cm}^{-1}$  does not change with time, indicating that it has not noticeably diffused into the polysiloxane layer (*i.e.*, it has not moved closer to the germanium interface). The carbon double bond stretching mode of

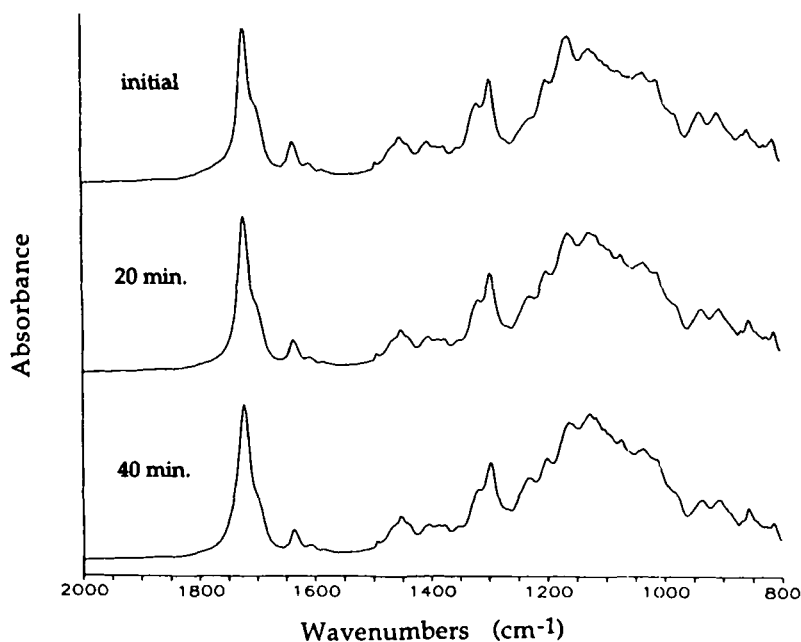


FIGURE 5 IR-IRS spectra of polyester cure on VTCS-coated Ge.

the vinyl group of the silane coupling agent at  $1602\text{ cm}^{-1}$  and the C—H bending mode of the methylene group is observed at  $1410\text{ cm}^{-1}$ . The largest absorption is observed in the region between  $1200\text{ cm}^{-1}$  and  $1000\text{ cm}^{-1}$ , indicative of the multi-layer polysiloxane structure of the coating. To determine whether or not the vinyl groups of the silane coating react during the cure reaction, the peak at  $1602\text{ cm}^{-1}$  was measured relative to the peak at  $1037\text{ cm}^{-1}$ , which is attributed to the antisymmetric stretching mode of Si—O—Si bonds of the coupling agent. The result of the analysis is shown in Figure 6. It is apparent that there is no significant decrease in the peak height ratio as a function of time which suggests little or no reaction of the vinyl groups of the VTCS in the silane-polyester interphase. After completion of the experiment, the element had to be soaked in chloroform for over 8 hours in order to remove the cured unsaturated polyester from the germanium. Infrared analysis of the fractured surface showed the presence of both polyester and siloxane, suggesting that chemical reaction at that interface was probable. Graft copolymerization probably takes place at the silane-matrix interface but is too little to be detected using the IR-IRS technique.

The internal reflection spectra of the OETCS coating in the presence of unsaturated polyester as a function of time at  $90^\circ\text{C}$  are shown in Figure 7. Two peaks are observed at  $910\text{ cm}^{-1}$  and  $990\text{ cm}^{-1}$  which are associated with the terminal vinyl groups of the OETCS and/or the terminal vinyl groups of the styrene in the polyester mixture. They

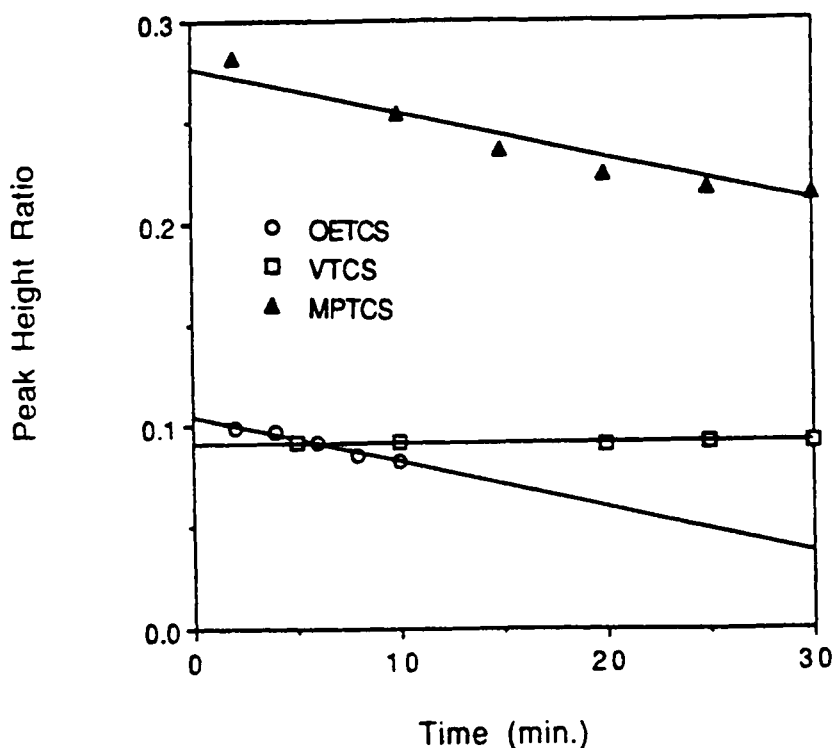


FIGURE 6 Peak height ratio versus cure time for reaction of silanes in the interphase.

decrease with time, indicating a net loss of unsaturation with time. Other peaks at 1630, 1500, 1450 and 1410  $\text{cm}^{-1}$  coincide with characteristics of polyester, styrene and OETCS and are not easily separable. In the initial spectrum, two peaks associated with the unsaturated polyester at 1720  $\text{cm}^{-1}$  and 1495  $\text{cm}^{-1}$  are detectable and represent non-reactive groups of the polyester and styrene. The carbonyl stretching mode at 1720  $\text{cm}^{-1}$  appears as a weak diffuse absorption band, and the peak attributed to the phenyl rings of the polyester and styrene appears at 1495  $\text{cm}^{-1}$ . As time proceeds, these peaks, as well as peaks most likely associated with the ester linkages of the polyester at 1298  $\text{cm}^{-1}$  and 1234  $\text{cm}^{-1}$ , are observed to increase in intensity. After ten minutes, the intensity of the carbonyl absorption of the unsaturated polyester at 1720  $\text{cm}^{-1}$  has reached its maximum. This indicates diffusion of the unsaturated polyester into the silane coating during the initial portion of the cure reaction. After twelve minutes, these absorption peaks have disappeared, apparently due to loss of contact between the curing unsaturated polyester and the silane-coated germanium element. At the end of the experiment, the cured polyester showed no resistance to removal from the germanium element.

The height of the peak at 1641  $\text{cm}^{-1}$ , associated with the carbon double bond stretching mode of the OETCS coating, was measured relative to the peak at 1118.5  $\text{cm}^{-1}$ , which is associated with the antisymmetric Si—O—Si stretching mode of the silane coating. The decrease in the peak height ratio is shown in Figure 6, indicating that there is reaction of the silane vinyls in the 0.06  $\mu\text{m}$  thick silane-polyester interphase created by the OETCS. When the thickness of the OETCS coating

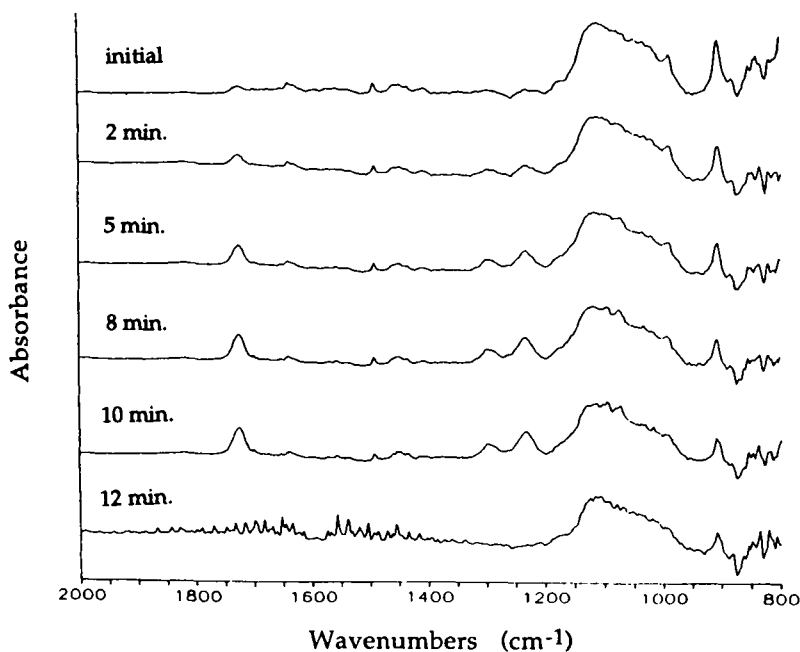


FIGURE 7 IR-IRS spectra of polyester cure on OETCS-coated Ge.

was increased to 0.18  $\mu\text{m}$ , no significant decrease in the peak height ratio was observed. These results suggest that the vinyls at or near the silane coating-polyester interface do react; however, those buried in the interior of the multilayer polysiloxane coating do not. After removal of the cured polyester from the silane-treated germanium, an IR spectrum was taken of the germanium surface. Characteristic peaks of the polysiloxane coating are observed at  $1641\text{ cm}^{-1}$ ,  $1454\text{ cm}^{-1}$ , and  $1100\text{ cm}^{-1}$  indicating that failure was within the siloxane interphase. Although weak in intensity, two peaks characteristic of the unsaturated polyester are also observed at  $1725\text{ cm}^{-1}$  and  $1495\text{ cm}^{-1}$ . This suggests that failure occurred in the interphase near the silane/polyester interface. We hypothesize that the interphase does not have sufficient strength to support the net internal stresses that arise as a result of swelling of the siloxane by polyester and shrinkage of the resin during the cure reaction.

The IR spectra for the  $\gamma$ -MPTCS-coated germanium in the presence of the unsaturated polyester at  $90^\circ\text{C}$  are shown in Figure 8. In the initial spectrum, peaks associated with both the  $\gamma$ -MPTCS-coating and the unsaturated polyester are observed, although the peaks associated with the polyester are extremely weak. The strong absorption around  $1720\text{ cm}^{-1}$  is a combination of the carbonyl peaks of the unsaturated polyester and the methacryloxysilane coupling agent. The carbon double bond stretching frequency and the  $\text{CH}_2$  bending mode of the terminal vinyl group of the  $\gamma$ -MPTCS are observed at  $1637$  and  $1170\text{ cm}^{-1}$ , respectively.

In order to analyze the reactivity of the methacryloxypropyl functional groups the height of the peak at  $1637\text{ cm}^{-1}$ , associated with the carbon double bond stretching

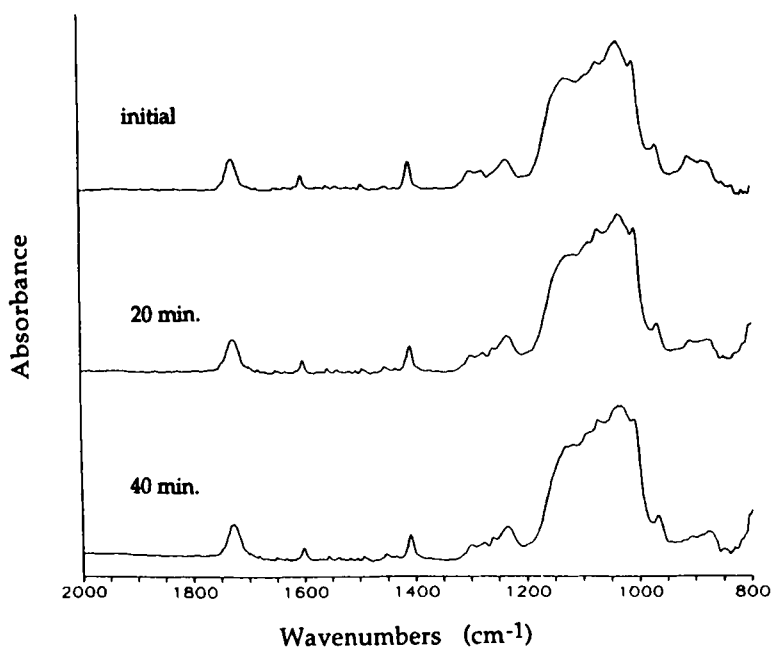


FIGURE 8 IR-IRS spectra of polyester cure on  $\gamma$ -MPTCS-coated Ge.

mode of the silane, was measured relative to the height of the peak at  $1128\text{ cm}^{-1}$ , which is associated with the antisymmetric stretching mode of the Si—O—Si bonds of the polysiloxane coating. Figure 6 shows a steady decrease in the peak height ratio as a function of time, suggesting that there is reaction of the methacryloxy groups of the silane coupling agent in the interphase. Another indication of reaction is the observed decrease in the peak at  $1170\text{ cm}^{-1}$ , which is attributed to the  $\text{CH}_2$  bending mode of the terminal vinyl groups. These observations are consistent with other reports in the literature on the reactivity of methacryloxy functional groups.<sup>7,27</sup> Two feasible reaction mechanisms can be envisioned; copolymerization of the silane vinyls with the unsaturated polyester/styrene mixture, and/or homopolymerization of the silane vinyls. Verification of these reactions would be the appearance of an absorption peak in the range of  $1750\text{--}1730\text{ cm}^{-1}$  from the formation of saturated carbonyl groups. This is not apparent in the spectra shown in Figure 8. The peak at  $1720\text{ cm}^{-1}$ , however, has a breadth of almost  $100\text{ cm}^{-1}$  at the base so that a weak saturated carbonyl peak would be difficult to see under the much stronger band. Since the  $0.2\text{ }\mu\text{m}$  coating of  $\gamma$ -MPTCS is comparable with the depth of penetration of the radiation, the amount of polymerization at the polyester/silane interface would be negligible compared with the total mass of carbonyl seen by the radiation, unless the diffusion of polyester into the coating was substantial. This does not appear to be the case since the band at  $1720\text{ cm}^{-1}$  is nearly constant. In a separate transmission IR experiment, a  $\gamma$ -MPTCS-coated silicon wafer was covered with a polystyrene/toluene solution and heated for one hour at  $90^\circ\text{C}$ . The carbonyl absorption peak was seen to shift from  $1720\text{ cm}^{-1}$  to  $1730\text{ cm}^{-1}$  indicating homopolymerization of the methacryloxy groups. While the results confirm the reactivity of the methacryloxy groups, the ratio of homopolymerization to copolymerization cannot be extracted from these data. One indication that copolymerization of the silane vinyls with the unsaturated polyester takes place is the difficulty of removing the cured unsaturated polyester from the silane-coated germanium. After 15 hours of immersion of the  $\gamma$ -MPTCS-coated element in chloroform the germanium element fractured near the silane/germanium interface. The solvent swelling stresses created at the interface were insufficient to break bonds between the germanium and the silane/polyester interphase, but strong enough to shear the germanium crystal.

In summary, the VTCS forms a relatively impermeable siloxane film on the fiber surface that probably reacts with the polyester at the VTCS/polyester interface; the OETCS and the polyester interdiffuse and correect, but form a mechanically weak interphase; the MPTCS and the polyester interdiffuse and correect to form a mechanically-strong interphase.

### Stress Transmission Across the Interphase

The magnitude of stress transmitted from the matrix to the reinforcing fibers (*i.e.*, the fiber efficiency) is controlled by the chemical bonding between components and the mechanical properties of the interphase. The embedded single fiber fragmentation test (ESFT) is one measure of the stress transmissibility.<sup>28</sup> In conjunction with the ESFT, optical microscopy was used to examine stress birefringence patterns and failure modes in the embedded single fiber specimens, and a finite element analysis was carried out to determine which mechanical properties of the interphase would control the observed failure modes.

Type V dogbone specimens were prepared using VTCS-, OETCS- and MPTCS-coated fibers embedded in an unsaturated polyester matrix in conformance with the requirements of ASTM D638. Samples were cast by using two glass plates on either side of an aluminium mold. One plate had a sand-blasted fill avenue that allowed the mold to be filled from the bottom up. A single glass fiber was positioned along the centre line, and the mold was filled with the unsaturated polyester-catalyst mixture using a syringe. Air bubbles were allowed to rise to the top of the mold and removed. The resulting single fiber composite was cured in a stepwise fashion at 80°C, 90°C and 120°C for one hour at each temperature and then cooled at 0.2°C/minute to room temperature. Upon removal from the mold, samples were sanded using fine grit sandpaper so that smooth, defect free surfaces were obtained. They were then tested in tension at a crosshead rate of 0.254 mm/min, and at room temperature and 60°C. Fragmentation of the fiber was continued to saturation and mean fragment length,  $l_m$ , was measured at the midpoint of the cumulative fragment length distribution. Critical length,  $l_c$ , and the average shear stress transmissibility,  $\langle \tau \rangle$ , were then calculated from the relationships:<sup>15</sup>

$$\langle \tau \rangle = \frac{\sigma_f d_f}{2l_c} = \frac{3\sigma_f d_f}{8l_m} \quad (4)$$

where  $\sigma_f$  is the fiber strength at the critical length and  $d_f$  is the average fiber diameter. A minimum debonding energy,  $G_d$ , was also calculated using the following equation:<sup>29</sup>

$$G_d = \frac{\sigma_f^2 d_f}{16E_f} \quad (5)$$

The fiber diameter,  $d_f = 13.0 \pm 0.1 \mu\text{m}$ , and the fiber strength at the critical length were determined as described in previous publications.<sup>15,28,29</sup>

A comparison of the cumulative distribution curves for four systems are shown in Figure 9. The bare fiber, MPTCS-coated and VTCS-coated systems exhibit narrow distributions of fragment lengths, closely approaching the dispersion expected from a shear lag model. This suggests "perfect" adhesion at the fiber surface with a fragment length limited by the shear strength of the interphase. The bare fiber system is shifted to the smallest mean fragment length suggesting the largest shear stress transmissibility. The OETCS-coated system exhibits a very broad distribution of fragment lengths with a large mean fragment length. This suggests slippage at or near the fiber/matrix interface and low shear stress transmissibility. In previous work it was found that there is no significant difference in strength between bare glass and silane-coated fibers until fiber lengths exceed 2 to 5 mm, so that the differences in the cumulative distribution curves are related primarily to the properties of the interphase and matrix.<sup>15,29</sup>

Equations (4) and (5) were used to evaluate the shear stress transmissibilities and the minimum debonding energies. The results are shown in Table III for the bare fiber system and MPTCS-, VTCS- and OETCS-treated systems. The shear stress transmissibility for the polyester-bare E-glass fiber composite,  $\tau = 51 \text{ MPa}$ , is in the range of the shear yield strength of the polyester matrix. The measured value of tensile yield strength of the matrix at 0.254 mm/min is equal to  $63.2 \pm 4.5 \text{ MPa}$ . Using a modified vonMises yield criterion, one calculates values of 37 MPa and 53 MPa for the shear yield strength of the polyester under conditions of no hydrostatic constraints (pure shear) and under



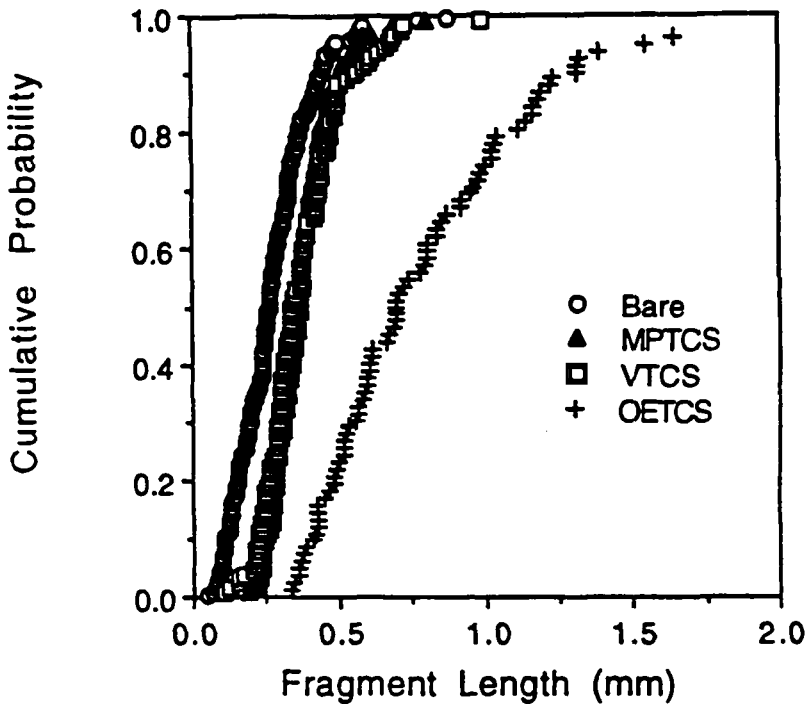


FIGURE 9 Cumulative probability versus fragment length for bare and silane-coated glass/polyester systems at room temperature.

the triaxial stress constraints extant at the fiber surface, respectively. The value of minimum debonding energy,  $G_d = 85 \text{ J/m}^2$ , is considerably lower than that found in previous studies<sup>29</sup> and results from the use of E-glass fibers that are much weaker than those used before (*i.e.*, estimated strengths in the range of 2,400–2,800 MPa for fibers 0.3 to 1.0 mm in length, compared with 3,200–3,800 MPa in previous work). In the region of the glass transition temperature of the polyester matrix, *i.e.*, 60°C, the value of  $\tau = 23 \text{ MPa}$  cannot be compared easily with the shear yield strength of the matrix, which is highly sensitive to the mode of testing and the constraints at the fiber surface.

TABLE III  
Shear Stress Transmissibility and Minimum Debonding Energy From ESFT  
(Unsaturated Polyester/E-glass fiber  $d_f = 13 \mu$ )

Silane	$T = \text{Room Temperature}$			$T = 60^\circ\text{C}$		
	$l_c(\text{mm})$	$\tau(\text{MPa})$	$G_d(\text{J/m}^2)$	$l_c(\text{mm})$	$\tau(\text{MPa})$	$G_d(\text{J/m}^2)$
Bare Fiber	0.35	51	85	0.72	23	70
MPTCS	0.49	35	77	0.63	26	73
VTCS	0.45	38	79	0.92	17	66
OETCS	0.93	17	66	0.97	16	65

The shear stress transmissibility for the OETCS coated system,  $\tau = 17$  MPa, is in the range expected for a friction-limited system and is consistent with the IR-IRS study showing that the interphase readily fractures under the triaxial stresses generated at the fiber surface. The value of  $\tau = 38$  MPa at room temperature for the VTCS-coated system is almost equal to the shear yield strength of unconstrained polyester, which might imply interphase failure further away from the fiber surface, on the polyester side of the VTCS/polyester interface. This is consistent with the IR-IRS study that showed very little interdiffusion of the polyester into the polysiloxane and a fracture surface containing both polyester and VTCS. The shear stress transmissibility for the MPTCS-coated material,  $\tau = 35$  MPa at room temperature, is similar to that of the VTCS-coated system, but retains its strength at 60 °C to a greater degree than that of the other two coated systems. The IR-IRS study confirms that the interphase is an interpenetrated mixture of the polyester and MPTCS and is well bonded to the E-glass surface.

In addition, single fiber tests were carried out on reactive dichloro- and monochlorovinylsilane-coated fibers (VMDCS, VDMCS and OEDMCS) and one system with no vinyl reactivity (ETCS). Results were similar to those described above, with the reactive vinylsilane coatings having shear stress transmissibilities in the range of 31–46 MPa, and non-reactive coatings in the range of 19–35 MPa. Results were sensitive to the concentration of the treating solution, which controlled the final coating thickness.

In all cases we believe the evidence indicates that the bonding between the E-glass surface and the chlorosilane is strong and that the level of stress transmission from the matrix to the fiber is controlled by the mechanical properties of the interphase and its interaction with the bulk matrix. At first glance it is surprising that the bare glass fiber system produces smaller fragment lengths at room temperature than those from silane-coated fibers. In any event, it is our view that calculated values of stress transmissibility should not be compared without a complete description of the mode of fracture at the broken fiber end and precise information on fiber strength at the critical length.

### Microscopic Observation of Fracture Modes

Single fiber composite samples under tension at room temperature and 60 °C were viewed under a microscope using polarized light. Three distinct modes of crack propagation from the broken fiber end were observed. One mode of failure is primarily interfacial (Figure 10). Two breaks in the fiber are seen and interfacial crack propagation has occurred. The advancing crack tips are observed as bright white spots near the fiber surface that have moved away from the initial fiber break. A very small amount of matrix failure at the fiber breaks is also observed. Interfacial failure occurred primarily in the OEDMCS, OETCS, VDMCS, VEDCS, and the 5% ETCS system. The birefringence sheaths, indicating stress build up near the fiber break, were seen to move away from fiber ends fairly quickly as the sample was deformed. Since the stress transmission is greater than that provided by mere friction, it is assumed that failure occurs by fracture of the weak interphase between the glass fibers and the polyester matrix.

A second mode of failure is primarily matrix cracking as shown in Figure 11. Cracks are observed to emanate from fiber breaks and propagate into the matrix, perpendicu-

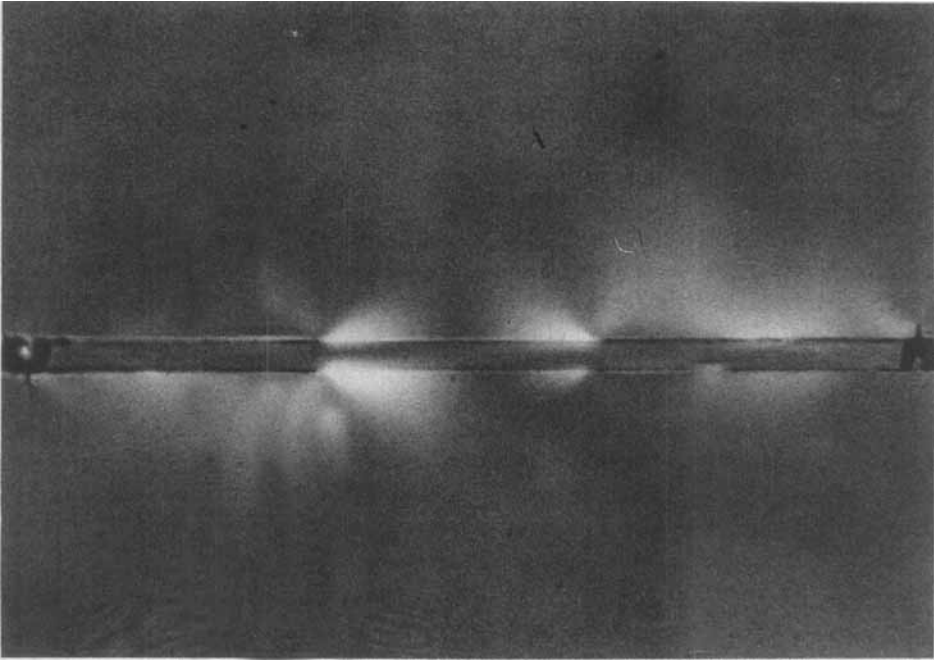


FIGURE 10 Fracture pattern of VDMCS-coated fiber embedded in unsaturated polyester.

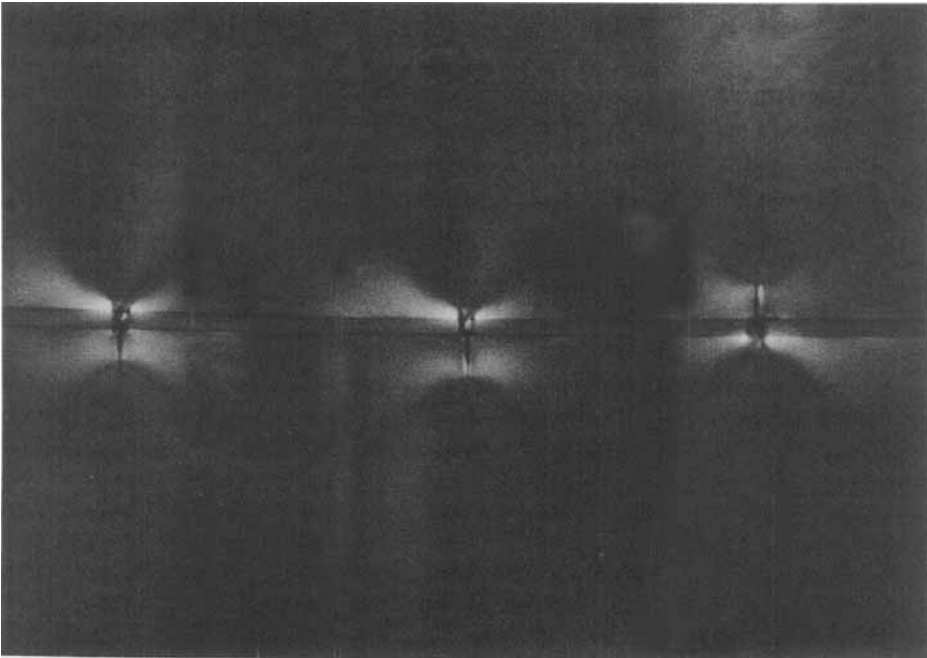


FIGURE 11 Fracture pattern of VTCS (5%)-coated fiber embedded in unsaturated polyester.

lar to the fiber and loading direction, with very little, or no, interfacial debonding. This failure mode was found to occur extensively in the system containing the E-glass fiber treated with the 5% VTCS solution and is an indication of a strong, tough interphase that is capable of resisting crack propagation; the limiting factor in this case is the fracture toughness of the matrix.

The third mode of failure is of a mixed nature, consisting of matrix crack propagation followed by interphasial debonding (Figures 12 and 13). In both the bare glass and MPTCS-treated systems a crack initiates at the fiber break and propagates into the matrix. At a specific strain level the matrix crack stabilizes and a further increase in strain causes interphasial crack propagation at the broken fiber end. The strain level at which this occurs appears to be a function of interphase properties and thickness. The MPTCS-treated system exhibits less interphasial cracking, at the same level of strain, indicating it is tougher than the interphase of pure polyester.

At 60°C the MPTCS-treated system exhibits extensive conical cracking of the matrix with little or no interphasial failure (Figure 14). This indicates that shear failure of the matrix is the primary mode of crack propagation. All other systems, including the bare glass, exhibited extensive interphasial failure at 60°C. The ETCS-treated system, in which there is no possibility of chemical reaction with the unsaturated polyester, showed extensive fiber slippage and, in some cases, no fiber fragmentation at all. The VTCS-treated systems from 5% and 10% coating solution concentrations exhibited mixed mode failure at 60°C.

The expression used to calculate stress transmissibility,  $\tau$ , (Equation (4)) is merely a statement of Newton's Third Law, assuming that the shear stress on the fiber surface is uniform along the fiber length. The calculated value of  $\tau$  is only a measure of the capacity of the matrix to transmit stress to a single embedded fiber. Since the mode of failure will depend upon the dynamic state of stress at points within the composite, one should view with caution attempts to compare values of  $\tau$  from different systems or to use such information to deduce composite properties.

### **Finite Element Analysis of Fracture Modes in an Embedded Single Fiber Composite**

A fuller understanding of the effects of an interphase on stress transmissibility and mode of fracture can result from a measurement of interphase properties and analysis of the state of stress in the composite. In order to guide future studies, a linear elastic axisymmetric finite element analysis of a single fiber composite was performed to determine the effects of fracture toughness, elastic modulus and thickness of an interphase on crack propagation from a broken fiber end.

The embedded single fiber specimen was modelled as a cylinder of matrix material surrounding an E-glass fiber with a distinct interphase. Perfect adhesion between all constituents and linear elastic behavior was assumed. Details of the finite element model and some initial results have been reported in a prior publication.<sup>16</sup> Some details of the mesh design were modified slightly when the need for greater refinement was called for.

The component elastic properties used in the analysis were:

$$\begin{array}{ll} \text{Fiber: } E_f = 72 \text{ GPa} & \nu_f = 0.22 \\ \text{Matrix: } E_m = 2.7 \text{ GPa} & \nu_m = 0.35 \end{array}$$

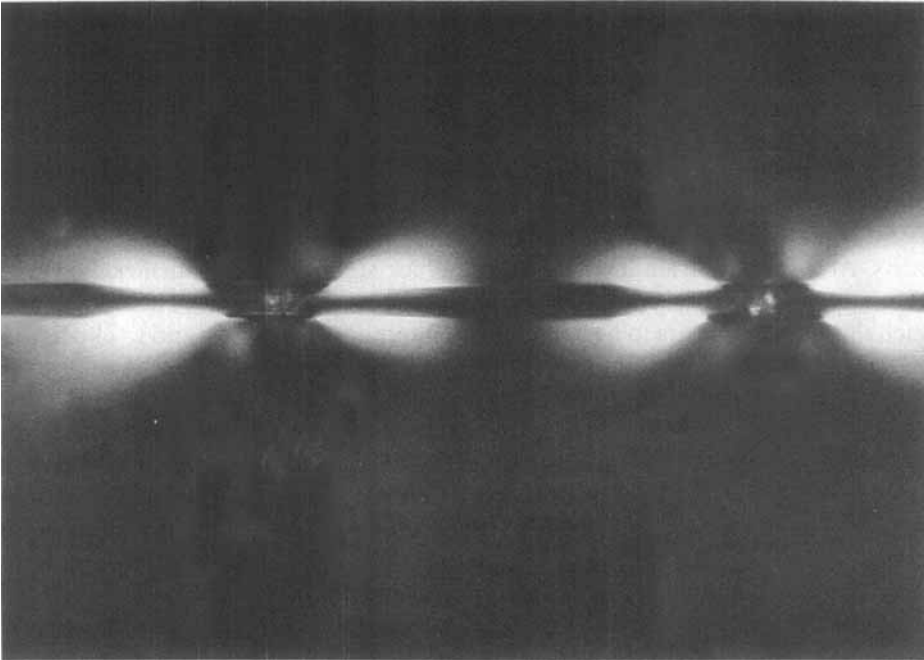


FIGURE 12 Fracture pattern of bare glass fiber embedded in unsaturated polyester.

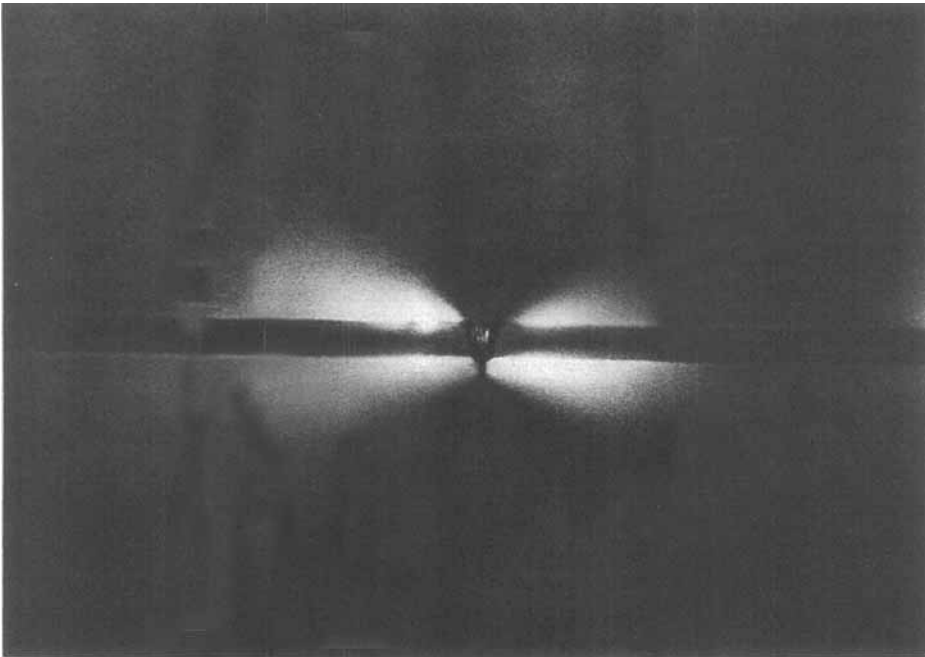


FIGURE 13 Fracture pattern of  $\gamma$ -MPTCS-coated fiber embedded in unsaturated polyester tested at room temperature.

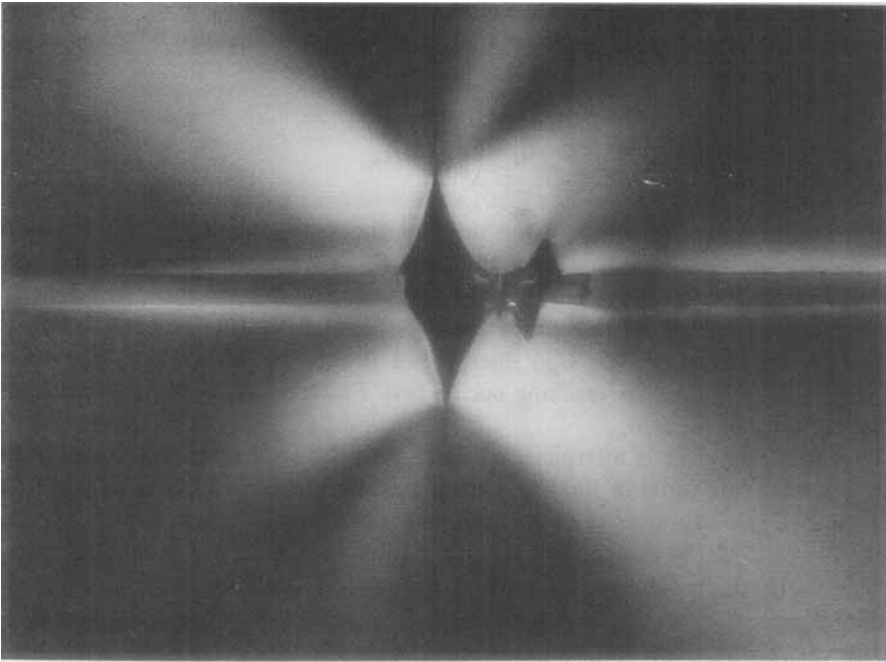


FIGURE 14 Fracture pattern of  $\gamma$ -MPTCS-coated fiber embedded in unsaturated polyester tested at 60 °C.

where  $E$  is Young's Modulus and  $\nu$  is Poisson's ratio. The modulus of the interphase,  $E_i$ , was varied between  $50 \geq E_i/E_m \geq 0.01$  and the effect of the Poisson ratio of the interphase,  $\nu_i$ , was studied at values of 0.2, 0.35 and 0.5. Interphase thicknesses of  $0.00625 d_f$ ,  $0.01875 d_f$  and  $0.03125 d_f$  were also considered.

For a specific set of material properties and interphase thickness, the fiber breakage, interphase debonding and matrix cracking were modelled by deleting mesh elements in the appropriate regions. Three sequences of events were studied:

1. Fiber breakage followed by matrix cracking perpendicular to the fiber axis.
2. Fiber breakage followed by interphase debonding parallel to the fiber axis.
3. Fiber breakage followed by matrix crack propagation and stabilization at a given crack length, followed by interphase debonding.

Upon deletion of the appropriate elements in the mesh, the elastic strain energy,  $U$ , of the composite at a fixed strain was calculated. An energy release rate,  $G$ , was then determined for each sequence from the relationship of  $G$  to the rate of change of elastic strain energy with crack area,  $A$ , at constant strain:

$$G = -(\delta U / \delta A)_\epsilon \quad (6)$$

A second order polynomial appeared to fit all situations adequately.

$$U = U_o - G_o A + b A^2 \quad (7)$$

$$G = G_o - 2b A \quad (8)$$

The initial strain energy release rate,  $G_o$ , was obtained by extrapolating to zero crack area at a composite strain,  $\epsilon$ . Since the analysis is linear,  $G$  values can be scaled to any strain,  $\epsilon$ , as follows:

$$G_\epsilon = \left(\frac{\epsilon}{\epsilon_0}\right)^2 (G)_{\epsilon_0}$$

Figure 15 illustrates the effect of the ratio of elastic moduli,  $E_i/E_m$ , on values of strain energy released due to matrix cracking,  $G_{mo}$ , interphase debonding,  $G_{io}$ , and the ratio of the two ( $G_{io}/G_{mo}$ ). Which of the two failure modes will occur first depends on the critical values of the strain energy release rate,  $G_c$ , for each mode of failure. When  $(G_{io}/G_{mo}) > (G_{ic}/G_{mc})$  interphasial debonding occurs first, and when  $(G_{io}/G_{mo}) < (G_{ic}/G_{mc})$  matrix cracking occurs first. Fracture will actually occur when either  $G_{io} = G_{ic}$  or  $G_{mo} = G_{mc}$ .

To examine the effect of interphase modulus, consider a matrix with a critical strain energy release rate equal to  $100 \text{ J/m}^2$ . When the interphase modulus is  $5.4 \text{ GPa}$  (i.e.,  $E_i/E_m = 2$ ),  $G_{mo} = 3411 \text{ J/m}^2$  at  $\epsilon = 0.1$ , and matrix cracking can occur at  $(100/3411)^{1/2} 0.10 = \epsilon = 0.017$  (1.7% elongation). When the interphase modulus is  $0.027 \text{ GPa}$  (i.e.,  $E_i/E_m = 0.01$ ),  $G_{mo} = 666 \text{ J/m}^2$  at  $\epsilon = 0.1$ , and matrix cracking can occur at  $\epsilon = 0.039$  (3.9% elongation). In the former case matrix cracking occurs first when  $G_{ic} > 66 \text{ J/m}^2$ , i.e.,  $(2250/3400)(100)$ , and in the latter case when  $G_{ic} > 210 \text{ J/m}^2$ .

Also plotted in Figure 15 is the effect of composite energy storage efficiency,  $\xi$ , defined as the ratio of the energy stored in the composite after fiber breakage to that of a composite containing a bare, unbroken fiber (no interphase).

$$\% \text{ Composite Efficiency } \xi = \frac{U_b}{U_u}(100)$$

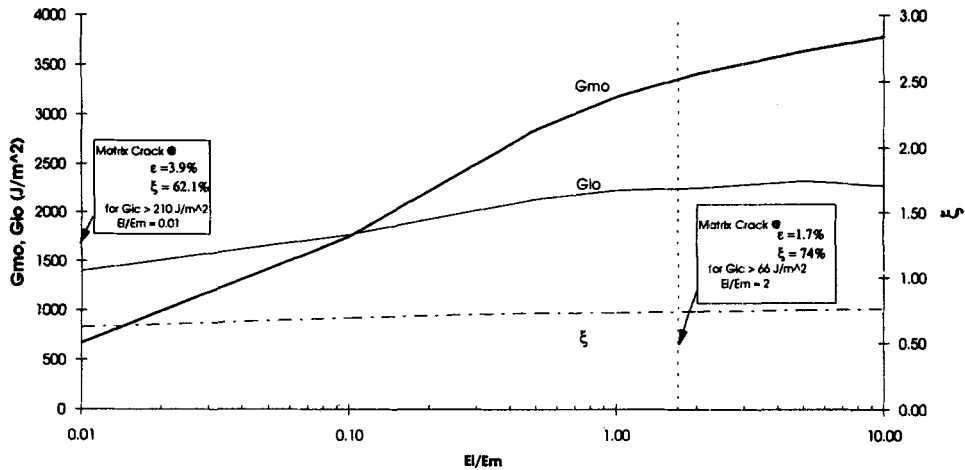


FIGURE 15 Strain energy release during interphase and matrix cracking in an embedded single fiber composite (elongation = 10%;  $G_{mc} = 100 \text{ J/m}^2$ ; interphase thickness =  $0.01875 d_f$ ).

As can be seen, the energy efficiency decreases as the interphase modulus decreases, *i.e.*, 74% when  $E_i/E_m = 2$  to 62% when  $E_i/E_m = 0.01$ . Thus, increased elongation before matrix cracking can be obtained with an appropriately designed interphase, but at the expense of efficiency in terms of the load bearing capacity of the composite.

Figure 16 illustrates the effect of matrix crack area on the strain energy released upon further crack propagation either in the matrix or along the interface. Consider the case of  $G_{mc} = G_{ic} = 100 \text{ J/m}^2$ . Matrix cracking will initiate at 1.6% elongation when  $G_{mc} = 100 \text{ J/m}^2$  and  $G_{io} > 69 \text{ J/m}^2$ . If the material is stressed to 2% elongation, the matrix will crack spontaneously, but would stabilize at  $G_{mo} = 2500 \text{ J/m}^2$  ( $\epsilon = 0.1$ ) at a crack area of  $12.4 \times 10^{-11} \text{ m}^2$  (a crack length of about  $2.6 \mu\text{m}$ ). There will not be interphase debonding since  $G_{ic} > 56 \text{ J/m}^2$ . If loading continues, the strain energy released by matrix cracking approaches that of interphasial debonding, becoming equal to it at a crack area of about  $32 \times 10^{-11} \text{ m}^2$ , corresponding to a crack length of  $5.5 \mu\text{m}$  and a composite elongation of 4.1% (*i.e.*,  $\epsilon = 0.1 (100/600)^{1/2}$ ). Beyond this point interphasial debonding will occur and will be favored until ultimate failure of the material, since  $(G_{io}/G_{mo})$  is now greater than  $(G_{ic}/G_{mc} = 1)$ .

A similar situation exists if interphasial debonding occurs first, (*i.e.*, when  $G_{ic} < 69$ ), but in this case the energy release rate for a matrix crack drops much more rapidly than that of the interphasial debond. In this case the weak interphase provides the maximum possible amount of crack tip blunting prior to ultimate failure of the composite.

Similar studies were done to determine the effect of interphase thickness. In general, the effect of an increase in interphase thickness is the same as reducing the modulus of the interphase. The greater the difference in the moduli of the interphase and matrix, the larger the effect. Over the range studied, the effect of a change in the ratio of Poisson's ratios was relatively small.

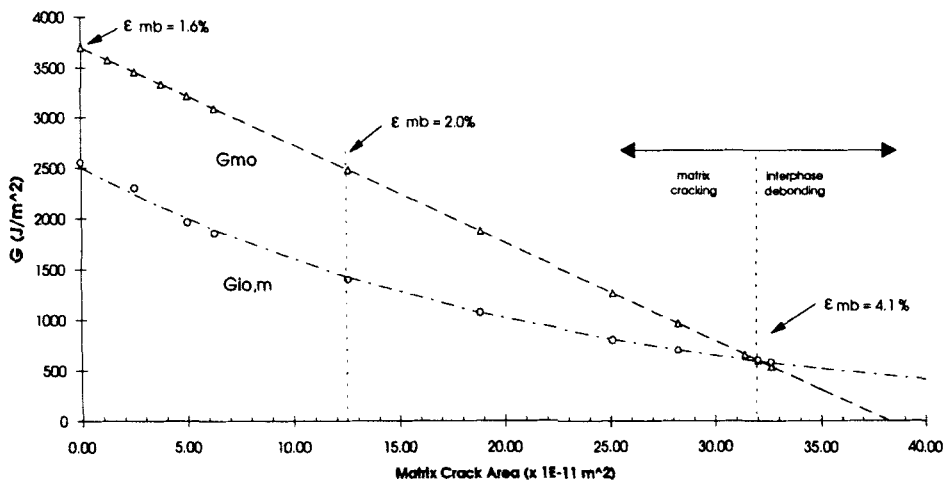


FIGURE 16 Strain energy release for interphase debonding after matrix cracking  $G_{io, m}$  at 10% elongation  $E_i/E_m = 1$ ,  $G_{mc} = G_{ic} = 100 \text{ J/m}^2$ , interphase thickness =  $0.0062 \text{ df}$ .



## CONCLUSION

In the three composite systems studied in detail, it is apparent that the chemical bonding of the silane coupling agent to the glass surface is strong and that the mechanical response of the composite is dependent upon the properties of the material in the vicinity of the fiber surface. In fabricating the polyester/silane coated fiber composite, the interaction between the polyester and the siloxane coupling agent creates an interphase zone with properties that are substantially different from the bulk matrix. A parametric study on a model composite of a single coated glass fiber embedded in an elastic matrix indicates that the thickness of the interphase and the relative moduli and fracture toughnesses of the interphase and matrix are the primary variables that control the failure modes following fiber fracture. The measurement of interphase moduli and ultimate properties is essential if one expects to tailor systematically the stiffness and toughness of composite materials.

## Acknowledgements

The authors wish to thank Dr. Josef Jancar for helpful discussions of all aspects of this work.

## References

1. A. T. DiBenedetto, D. A. Scola, *J. Colloid & Interface Sci.* **74**, 150 (1980).
2. D. Pawson, F. R. Jones, "The Role of Oligomeric Silanes on the Interfacial Shear Strength of AR Glass-Vinyl Ester Composites", in *Interfacial Phenomena in Composite Materials*, **89**; F. R. Jones, Ed. (Butterworths, Boston, 1989), p. 188.
3. M. E. Schrader, I. Lerner, F. J. D'Oria, *Modern Plastics* **45**, 195 (1967).
4. L. H. Lee, *J. Colloid & Interface Sci.* **27**, 751 (1968).
5. J. Shieh, T. J. Hsu, *Polym. Eng. Sci.* **32**, 335 (1992).
6. D. Lee, C. D. Han, *J. Appl. Polym. Sci.* **33**, 419 (1987).
7. H. Ishida, J. L. Koenig, *J. Polym. Sci., Polym. Phys. Ed.* **17**, 615 (1979).
8. G. H. Wagner, D. L. Bailey, A. N. Pines, M. L. Dunham, D. B. McIntire, *Ind. Eng. Chem.* **45**, 367 (1953).
9. H. A. Clark, E. P. Pleuddmann, *Modern Plastics* **409**, NO. 6, 133 (1963).
10. O. K. Johansson, F. O. Stark, G. E. Vogel, R. M. Fleischmann, *J. Comp. Mat.* **1**, 278 (1967).
11. A. Ahagon, A. N. Gent, E. C. Hsu, "On Bonding of Rubber to Glass", in *Adhesion Science and Technology*, L. H. Lee, Ed. Plenum Press, NY, 1975).
12. J. L. Koenig, P. Shih, *J. Colloid & Interface Sci.* **36**, 247 (1971).
13. S. W. Morrall, D. E. Leyden, "Modification of Siliceous Surfaces with Alkoxysilanes From a Nonaqueous Solvent", in *Silanes, Surfaces and Interfaces*, D. E. Leyden, Ed. (Gordon and Breach Science Pub., Ny, 1986), pp. 501–524.
14. A. Garton, *Polym. Composites* **5**, 258 (1984).
15. A. T. DiBenedetto, P. J. Lex, *Polym. Eng. Sci.* **29**, 543 (1989).
16. A. DiAnselmo, M. L. Accorsi, A. T. DiBenedetto, *Composites Sci. & Tech.* **44**, 215 (1992).
17. M. R. Kamal, S. Sourour, M. Ryan, *SPE ANTEC Tech. Paper* **19**, 187 (1973).
18. K. Lem, C. Dae Han, *Polym. Eng. Sci.* **24**, 175 (1984).
19. C. D. Han, K. W. Lem, *J. Appl. Polym. Sci.* **28**, 3155 (1983).
20. K. W. Lem, C. D. Han, *J. Appl. Polym. Sci.* **28**, 3185 and 3207 (1983).
21. E. L. Rodriguez, *Polym. Eng. Sci.* **31**, 1022 (1991).
22. J. Shieh, T. J. Hsu, *Polym. Eng. Sci.* **32**, 335 (1992).
23. H. Ng, I. Manas-Zloczower, *Polym. Eng. Sci.* **29**, 1097 (1989).
24. N. J. Harick, *Internal Reflection Spectroscopy* (Harrick Scientific Corp., NY, 1987), p.92.
25. A. Garton, private communication.
26. S. M. Connelly, "The Effect of Silane Treatments on Interphase Properties of a Glass Fiber Reinforced Unsaturated Polyester", Ph.D. Thesis, University of Connecticut, pp. 66–67, 84–85 (1993).
27. O. K. Johansson, F. O. Stark, G. E. Vogel, R. M. Fleischmann, *J. Comp. Mat.* **1**, 278 (1967).
28. W. A. Fraser, F. H. Ancker, A. T. DiBenedetto, B. Elberli, *Polymer Comp.* **4**, 238 (1983).
29. A. T. DiBenedetto, *Comp. Sci. Tech.* **42**, 103 (1991).